

An accurate equation of state for the one component plasma in the low coupling regime.

Jean-Michel Caillol

Laboratoire de Physique Théorique

CNRS (UMR 8627), Bât. 210

Université de Paris-Sud

91405 Orsay Cedex, France

Dominique Gilles

CEA/DSM/Institut de Recherche sur les lois Fondamentales de l'Univers

CE Saclay

91191 Gif sur Yvette Cedex, France^y

(Dated: February 22, 2024)

Abstract

An accurate equation of state of the one component plasma is obtained in the low coupling regime $0 < \Gamma < 1$. The accuracy results from a smooth combination of the well-known hypernetted chain integral equation, Monte Carlo simulations and asymptotic analytical expressions of the excess internal energy u . In particular, special attention has been brought to describe and take advantage of finite size effects on Monte Carlo results to get the thermodynamic limit of u . This combined approach reproduces very accurately the different plasma correlation regimes encountered in this range of values of Γ . This paper extends to low Γ 's an earlier Monte Carlo simulation study devoted to strongly coupled systems for $1 < \Gamma < 190$ (J.-M. Caillol, J. Chem. Phys. 111, 6538 (1999)). Analytical fits of $u(\Gamma)$ in the range $0 < \Gamma < 1$ are provided with a precision that we claim to be not smaller than $p = 10^{-5}$. HNC equation and exact asymptotic expressions are shown to give reliable results for $u(\Gamma)$ only in narrow intervals, i.e. $0 < \Gamma < 0.5$ and $0 < \Gamma < 0.3$ respectively.

PACS numbers: 52.65.-y, 52.25.Kn, 52.27.Aj

^Electronic address: Jean-Michel.Caillol@th.u-psud.fr

^yElectronic address: Dominique.Gilles@cea.fr

I. INTRODUCTION

The aim of this paper is to obtain the equation of state (EOS) of a plasma in the low coupling regime with a high precision. In this regime standard Monte Carlo (MC) and Molecular Dynamics simulations techniques must be handled with care due to huge finite size effects and, in the other hand, the ideal gas approximation or more elaborated analytical expressions commonly used are valid only but asymptotically, for very small values of the coupling parameters. Such thermodynamic conditions are relevant for many astrophysical or laboratory plasmas hydrodynamics applications.

However we shall restrict ourselves to the well known one-component plasma (OCP) model, which consists of identical point ions with number density n , charges Ze , moving in a neutralizing background, electrons for instance, where $n = N/V$, N number of particles, volume of the system [1]. In the very low coupling regime, the virial expansion supplemented by well documented resummation methods, as the well-known Debye-Huckel (DH) theory [2] and its extensions (see e.g. Cohen [3] and, more recently, Ortner [4] expansions for instance) give reliable results. In the low to intermediate coupling regimes the HyperNetted Chain (HNC) integral equation [5] must be solved numerically. Finally, in the strong correlation regime, the OCP has also been extensively studied by Monte Carlo and Molecular Dynamics simulations for three decades, see e.g. [1, 6, 7, 8, 9, 10, 11] and references cited herein.

In the more recent of these references one of us has determined the thermodynamic limit of the excess internal energy per particle $u_{N \rightarrow \infty}$ of the OCP with a high precision by means of MC simulations in the canonical ensemble within hyperspherical boundary conditions [10, 11] for $1 \leq \Gamma \leq 190$. We recall that in the thermodynamic limit, i.e. for an infinite system of particles, the thermodynamics properties of the model depend solely on the coupling parameter $\Gamma = (Ze)^2/a_i$ ($\beta = 1/kT$, k Boltzmann constant, T temperature, and a_i the ionic radius defined by $4\pi n a_i^3/3 = 1$), whereas, for a finite sample, an additional dependance on the number of particles N remains. In paper [11], henceforth to be referred to as "I", special attention has been brought to describe and take advantage of such finite size effects on the energy $u_N(\Gamma)$ to get its thermodynamic limit $u_{N \rightarrow \infty}$, using all facilities of work stations available at that time.

Recently we have also performed extensive MC simulations of the related Yukawa One-Component Plasma (YOC-P), i.e. a system made of N identical point charges Ze interacting

via an effective Yukawa pair-potential $v(r) = (Ze)^2 \exp(-r/\lambda_D)/r$, where λ_D is the so-called screening parameter [12], not to be discussed however in this work. For the OCP and the YOCP as well, in the low β regime, the Debye length (i.e. the correlation length associated with charge fluctuations) becomes of the order or much larger than the size of the simulation box, yielding huge finite size effects on $u_N(\beta)$. Therefore, despite these numerous studies and amount of work it appears that hydrocode applications using the combination of databases and tests coming from various techniques can be affected by numerical instabilities in the transition regime, around $\beta = 1$. With nowadays computers it is now possible to explore this range of small β values with the help of performant simulation techniques and to obtain such precise results so that they can be considered as the reference ones to be used in many applications dealing with degenerate astrophysical or laboratory plasmas. We also examine carefully in this paper the connection between MC and first principle analytical or HNC results for $\beta \leq 1$. We have thus explored and precised the domain of validity of each of these methods. It turns out to be necessary to combine all of these approaches to obtain a continuous representation of $u_{N=1}(\beta)$ in the range $0 \leq \beta \leq 1$. Finally we extract from these combined approaches the best possible analytical representation for $u_1(\beta)$.

Our paper is organized as follows. Next section is devoted to a brief presentation of the main features of low β expansions (Section IIA), the HNC integral equation (Section IIB) and the rather unusual but efficient MC technique used in this paper (Section IIC). Note that we have redone, by passing, extremely accurate HNC calculations and obtained new tests of HNC data, presented in Section IIB. In Section III we present and discuss our MC simulations. Fits of the data are described in details and widely illustrated. Finally conclusions are drawn in Section IV.

II. LOW β CALCULATION METHODS

The interval $0 \leq \beta \leq 1$ covers various correlation regimes from no correlation ($\beta = 0$, i.e. the ideal gas) to an intermediate correlated regime ($\beta = 1$, no oscillation or structure in the pair correlation functions). In any case, the long-range nature of the interaction potential between two ionic charges causes Mayer graphs to diverge [1]. A field theoretic diagrammatic representation of cluster integrals has been proposed recently in [4] to avoid complicated chain resummations in an attempt to treat the β expansion of the classical

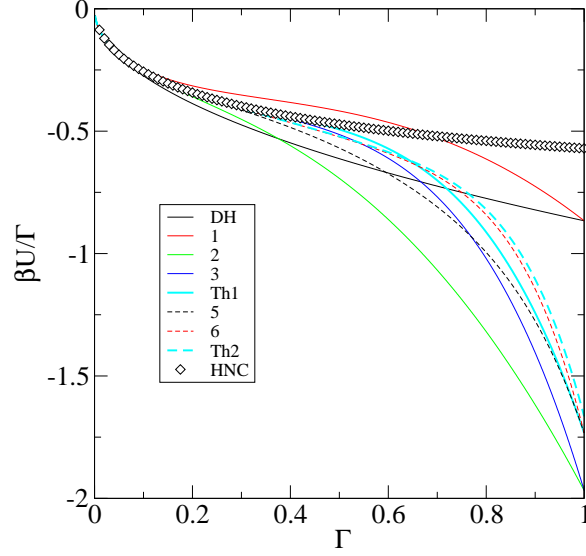


FIG. 1: Reduced excess energy $\beta U/\Gamma$ versus Γ . Diamonds: HNC, black solid line: DH, thick cyan solid line: Th1 approximation (2.1a), thick cyan dashed line: Th2 approximation (2.1b), other curves represent the successive orders of expansion (2.1).

Coulomb system in a more controlled and systematic way. In this interesting paper the new expansion obtained by the author improves earlier and seminal analytical results of Cohen et al. [2, 3] obtained by traditional diagrammatic expansions and resummations. From this theoretical analysis it turns out that the physics in this small interval $0 < \Gamma < 1$ is extremely complicated and exhibits many different correlation regimes, even more than in the widely studied region $1 < \Gamma < 190$ [1, 6, 7, 8, 9, 10, 11]. The low Γ expansions obtained by Cohen et al. and Ortnner for $u_1(\Gamma)$ converge to the HNC results only for $0 < \Gamma < 0.2$ as apparent in figure 1. For higher values of Γ these asymptotic expressions do not seem to converge at all and, moreover, the high order terms of the expansions do not improve the results of the lower orders. Anticipating the results of sections IIB and IIC and, as can be observed in figure 2, the HNC data deviate from our MC results as soon as $\Gamma > 0.5$. It results from this sketchy discussion that we must distinguish three different regimes of correlations in the interval $0 < \Gamma < 1$, and we confess that this complexity motivated the present study.

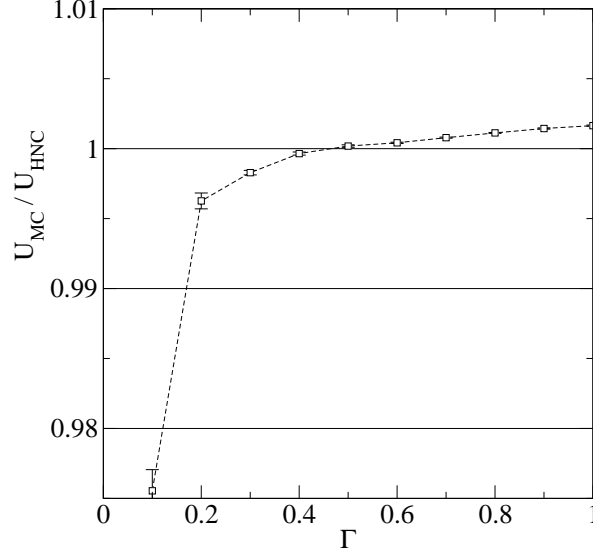


FIG. 2: Ratio of MC excess energies to HNC results versus Γ in the low coupling regime.

A. Cohen and Ornstein analytical expansions

In ref. [4] Ornstein has developed an effective method based on the Hubbard-Stratonovich (HS) transformation and field theoretical approaches to calculate the free energy of classical Coulomb systems in the low regime [13, 14, 15]. The HS transform was used to obtain the EOS of a classical plasma and notably that of the OCP. The non-trivial part of the Helmholtz free-energy density was derived up to order Γ^6 , improving on the previous results of Cohen et al. at order $\Gamma^{\frac{9}{2}}$, obtained by a method of resummation of diverging diagrams. The author gives an analytical representation of the excess internal energy u of the OCP, valid at low Γ , without however any estimation of the error. It reads as,

$$u(\Gamma) = p_0 \Gamma^{-3/2} + p_1 \Gamma^{-3} \ln \Gamma + p_2 \Gamma^{-3} + p_3 \Gamma^{-9/2} \ln \Gamma + p_4 \Gamma^{-9/2} \quad (2.1a)$$

$$+ p_5 \Gamma^{-6} \ln^2 \Gamma + p_6 \Gamma^{-6} \ln \Gamma + p_7 \Gamma^{-6} \quad (2.1b)$$

with the constants, $p_0 = \frac{1}{3} \sqrt{\frac{2}{\pi}}$, $p_1 = -\frac{1}{9}$, $p_2 = -\frac{1}{8} (9 \ln 3 - 8)$, $p_3 = \frac{1}{27} \sqrt{\frac{2}{\pi}}$, $p_4 = 0.2350$, $p_5 = -\frac{1}{81}$, $p_6 = 2.0959$, $p_7 = 0.0676$ and $C_E = 0.57721566$ the Euler constant. Expression 2.1 (to be referred to as Th2 henceforth) improves on that given by Cohen et al. (to be referred to as Th1 henceforth) [3], which corresponds to line 2.1a, while the additional terms are those of line 2.1b. We recognize that the first term ($\frac{1}{3} \sqrt{\frac{2}{\pi}} \Gamma^{-3/2} = 2$) is exactly the well known Debye-Huckel (DH) contribution. Figure 1 displays the results of the reduced excess energy u^* versus Γ at successive orders in the

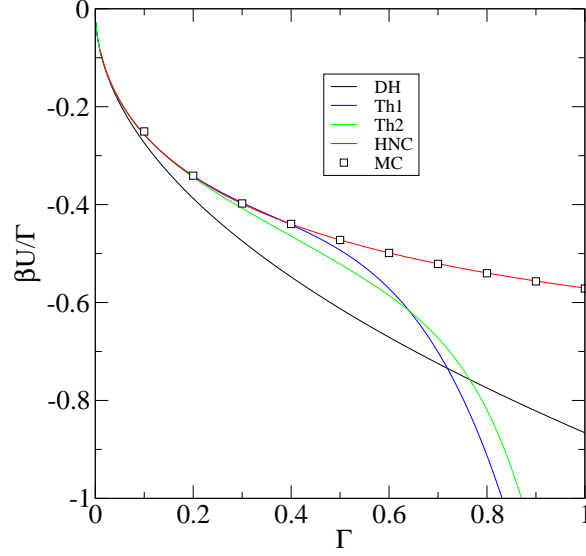


FIG. 3: Reduced excess energy $\beta u = \beta U/\Gamma$ versus Γ . Squares: MC (the symbols are larger than error bars), black line: DH, red line: HNC, blue line: Th1 approximation (2.1a), green line: Th2 approximation (2.1b).

expansion 2.1. A close examination of the figures reveals that the DH approximation is nearly exact up to $\Gamma = 0.05$, in the sense that higher order contributions do not change the result. A comparison with HNC results, which are supposed to be nearly exact at least up to $\Gamma = 0.5$ (this point will be fully discussed in next section), shows the convergence of the expansions Th1 and Th2 to HNC at $\Gamma = 0.3$ and $\Gamma = 0.2$ respectively. However we do not observe any trend of convergence of these expansions for $\Gamma > 0.4$. We also notice that the additional terms given by Orntner (cf equation 2.1b) lead to an oscillatory behavior rather than to an improved convergence radius. We suspect some misprints in the reported p_n for $n = 5, 6, 7$ since the functional dependence of 2.1 is undoubtedly correct.

B. HNC method and tests

1. Method

We have redone high precision HNC calculations for a hundred of values of Γ in the range $(0; 1)$ (see figures 1 and 3); additional calculations were also done for some higher values of the coupling parameter, in the range $1 < \Gamma < 10$, see figure 4. We used the Ng method [5] with the following control parameters: the pair correlation functions (direct and non-direct

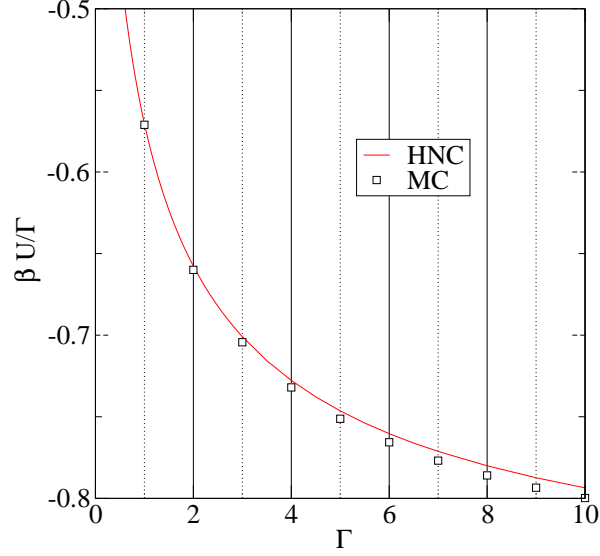


FIG. 4: Comparison between HNC (red line) and MC data (squares, present work and previous results, see ref.[11]) for the reduced excess energy $\beta U/T$ versus Γ from 1 to 10.

respectively) $c(r)$ and $h(r)$, as well as their Fourier transforms $s(k)$ and $\hat{h}(k)$, were tabulated on grids of $N = 2^M$ points with $M = 20$ in order to make use of fast Fourier transforms with intervals of $r = 0.001$ and $k = 2\pi/N \approx 610^{-3}$ in direct and Fourier space respectively. The dimensionless energies were computed according the formulae [1]

$$\frac{u^{(r)}}{k_B T} = \frac{3}{2} \int_0^{Z_1} dr r h(r); \quad (2.2a)$$

$$\frac{u^{(k)}}{k_B T} = \frac{3}{2} \int_0^{Z_1} dk \hat{h}(k); \quad (2.2b)$$

where the distances "r" are measured in the units of the ionic radius a_i and the wave numbers k in units of a_i^{-1} . The comparison of these two estimations $u^{(r)}$ and $u^{(k)}$ of the energy, which of course should be equal, give an idea on the relative precision of the numerical resolution of HNC, typically about 10^{-12} at $\Gamma = 0.01$ and 10^{-13} at $\Gamma = 0.1$. Another useful test is to check the Stillinger-Lovett (SL) sum rules; recall briefly the two first SL rules (the third one should not be satisfied by HNC [1])

$$\frac{3}{2} \int_0^{Z_1} dr r^2 h(r) = -1; \quad (2.3a)$$

$$\frac{3}{2} \int_0^{Z_1} dr r^4 h(r) = -\frac{2}{\Gamma}; \quad (2.3b)$$

With the control parameters given above the SL rules were satisfied with a relative precision of about 10^{-13} .

TABLE I: First five Cohen-O rtner coefficients (cf Eq. (2.1), first line) compared to the correspondent coefficients of the fits of the energy $u(r)$ for HNC and MC data. Second line : HNC, 7 parameters, $p_0 = \frac{p}{3} = 2$ fixed to its DH value. Third line : HNC, 8 parameters. Last line : MC data in the range $0.4 \leq r \leq 1$, 5 parameters ($p_5 = p_6 = p_7 = 0$).

| p0 | p1 | p2 | p3 | p4 | Method |
|--------------|--------------|--------------|--------------|--------------|---------|
| 0.8660254038 | 1.1250000000 | 1.1017662315 | 2.9228357378 | 0.2350000000 | O rtner |
| 0.8660254038 | 1.1127645260 | 1.0636075255 | 3.1960177420 | 1.4236810385 | HNC DH |
| 0.8658509448 | 1.0967358264 | 1.0224523661 | 2.9765709164 | 1.1861133643 | HNC |
| 0.8409025523 | 0.5198391670 | 0.0001985314 | 0.1402132305 | 0.2697081277 | MC |

TABLE II: Same as in Table I

for the last 3 parameters p_5, p_6, p_7 of the fit of HNC data.

| p5 | p6 | p7 | Method |
|--------------|--------------|--------------|---------|
| 5.062500000 | 2.0959000000 | 0.0676000000 | O rtner |
| 0.5868725967 | 2.1982700902 | 2.7828599024 | HNC DH |
| 0.5093239388 | 1.9531860886 | 2.5039620685 | HNC |

2. Fits

We used the functional form of O rtner asymptotic expression 2.1 to fit the HNC data for $u(r)$ in the interval $0.4 \leq r \leq 1$. We are left with a eight parameters fit (i.e. the p_i for $i = 0; \dots; 7$) or a seven parameters fit, if p_0 is fixed to its Debye value $p_0 = \frac{p}{3} = 2$. The values found for the p_i are given in the Tables I and II. For the eight parameters fit the maximum deviation of the fit from the HNC data is $7.3 \cdot 10^{-7}$ with a mean deviation of $1.9 \cdot 10^{-7}$, while for the seven parameters fit these deviations are $1.3 \cdot 10^{-6}$ and $3.3 \cdot 10^{-7}$ respectively. Some comments are in order.

Firstly, for $0.1 \leq r \leq 1$ the estimations of $u(r)$ in the framework of HNC, Cohen et al. and O rtner theories all coincide with an absolute precision of the order of $1 \cdot 10^{-4}$, as apparent in table III. These conclusions are also true for DH approximation.

The agreement between HNC energies and that predicted by Cohen et al. expression (cf Fig. 3 and table III) differ by less than $2 \cdot 10^{-3}$ in the range $0.4 \leq r \leq 0.8$.

Note that the apparent discrepancies between the p_i of the t of HNC and the "exact" coefficients of Cohen expansion do not spoil the excellent agreement between the two approaches.

The agreement between HNC energies and that predicted by Othner et al. expression (cf. Fig. 3 and table III) differ by less than $2 \cdot 10^{-3}$ in the range $0 \leq \beta \leq 0.2$.

From these remarks we conclude that HNC is, as expected, exact in the low coupling regime at least up to $\beta = 0.3$. Moreover DH theory cannot be trusted for $\beta \leq 0.1$, Cohen et al. expression can be used confidently as it stands for $\beta \leq 0.3$ and, unexpectedly, the additional orders in the asymptotic expression obtained by Othner do not improve, unfortunately, on Cohen results. We suggest to reexamine the details of the calculations of reference [4]. The functional dependence in β of equation (2.1) is probably correct but misprints in one of the p_i for either $i = 5, 6$ or $i = 7$ are likely.

C. MC theoretical background

MC simulations are not well adapted to the low coupling regime for two reasons. First, since the configurational energies are small, the convergence of the MC process is slow. Secondly, in the case of the OCP considered here, the Debye length $\lambda_D = \sqrt{\frac{\epsilon_0 k_B T}{n e^2}}$ diverges as $\beta \rightarrow 0$ and thus becomes larger than the (finite) size of the simulation box, which entails severe finite size effects. To use the MC method for obtaining very precise results for the OCP in the range of $\beta \leq 1$ is therefore a real challenge. Some comments on our methodology seem to us worthwhile.

Our simulations were performed in the canonical ensemble within hyperspherical boundary conditions. The particles are thus confined on the surface of a 4D sphere S^3 of radius R and the plasma pair potential between ions is simply the Coulombic interaction in this geometry. The latter has a simple analytical expression which allows high precision computations in contrast with the usual technique of Ewald summations where the potential is poorly determined at short distances. The theoretical background of this method has been already described in details in previous works [10, 11] and will not be rediscussed here. We only extract from these previous theoretical considerations the following point. It turns out that DH equation (i.e. Helmholtz equation) can be solved analytically in S^3 which yields the

exact finite size dependence of the excess internal energy in this approximation and therefore in the low coupling limit. One finds that at the leading order

$$u_N(\beta) - u_1(\beta) \sim N^{-2/3} \text{ for } \beta \rightarrow 0 \text{ and } N \rightarrow 1 : \quad (2.4)$$

Of course this behavior in only asymptotic and sub-leading terms in $N^{-2/3}$, $N^{-2/3}$ must be taken into account if N is not large enough. For couplings $\beta \leq 3$ we shown in paper I that we rather have $u_N(\beta) - u_1(\beta) \sim N^{-1}$. This remark yields the correct procedure : for a given parameter perform MC simulations for different number of particles N and take advantage of the scaling relation 2.4 to obtain the thermodynamic limit $u_1(\beta)$. The estimation of the statistical errors on the $u_N(\beta)$ and the extrapolated thermodynamic limit $u_1(\beta)$ is also described in details in I. However, by contrast with refs [10, 11] devoted to the strong correlation regime ($\beta \rightarrow 190$), present work only the small couplings are considered. In order to test the validity of HNC, notably in the range $0.3 \leq \beta \leq 1$ with an error of $1:10^{-4}$ we were led to perform huge Markov chains and consider very large systems up to $N = 51200$ particles in order to reach the scaling region where 2.4 applies. Since HNC and Cohen asymptotic forms for u differ by less than $1:10^{-4}$ in the range $0 \leq \beta \leq 0.3$ we can claim (as will be discussed in details below) an overall maximum error of $1:10^{-4}$ for the dimensionless $u = \beta U/N$ in the whole interval $0 \leq \beta \leq 1$.

Some additional simulations in the transition region to high correlation regime $\beta \approx 10$ were also performed to make contact with our previous results.

III. MC DATA ANALYSIS AND FITS

A. Data analysis

We adopted the same procedure as the one described in reference I. The MC simulations were performed using the standard Metropolis algorithm to build Markov chains in the canonical ensemble. In the small regime, $0 \leq \beta \leq 1$, where finite size effects are tremendously important, we considered much larger systems than before. In order to get the thermodynamic limit (TL) of the excess internal energy for each value of β , we performed simulations for samples of $N = 100; 200; 400; 800; 1600; 3200; 6400; 12800; 25600$; and 51200 particles. The cumulated reduced excess energy (CREE) $U(\beta; N) = \beta U/N$ at coupling β and

TABLE III: M is the dimensionless energy $u_N(\rho)$ of the OCP as a function of ρ for MC (with error bars), HNC, Cohen, and Ortnner approximations.

| | MC | HNC | Cohen | Ortnner |
|-----|---------------|------------|------------|-------------|
| 0.1 | 0.25117 (34) | 0.25688548 | 0.25677226 | 0.25699174 |
| 0.2 | 0.34111 (17) | 0.34238929 | 0.34127338 | 0.34436859 |
| 0.3 | 0.397693 (64) | 0.39837711 | 0.39608173 | 0.40761777 |
| 0.4 | 0.439323 (53) | 0.43968253 | 0.44115547 | 0.46432208 |
| 0.5 | 0.472172 (42) | 0.47208481 | 0.49302326 | 0.521520956 |
| 0.6 | 0.498715 (21) | 0.49850618 | 0.57144385 | 0.58565711 |
| 0.7 | 0.521064 (20) | 0.52064202 | 0.70120487 | 0.67244493 |
| 0.8 | 0.540173 (15) | 0.53956586 | 0.91276540 | 0.81996338 |
| 0.9 | 0.556823 (30) | 0.55600050 | 1.2425017 | 1.1053739 |
| 1.0 | 0.571403 (24) | 0.57045534 | 1.7327877 | 1.6651877 |

number of particles N , was computed as the cumulated mean over M successive configurations "i" of the Markov chains as

$$\overline{u_N; (M)} = \frac{1}{M} \sum_{i=1}^M \frac{V(i)}{N} \quad (1 \leq M \leq n_{\text{conf}}); \quad (3.1)$$

We generated MC chains of $n_{\text{conf}} = 4 \cdot 10^9$ configurations after thermal equilibration, for all systems up to $N = 25600$ particles. The reason was to reach a stable plateau for the CREE and to reduce statistical errors. These two points will be illustrated further. For $N = 25600$ such long chains result in the mixing of 5 independent chains, each one corresponding to half a month of CPU time. Thus the $N = 25600$ value of the excess energy represent a 2 months and a half calculation. For $N = 12800$ the total duration was 2 months, with two independent chains. For comparison a $N = 800$ simulation is performed in 2 days in a unique chain. One day is enough for a $N = 400$ simulation. These calculations have been performed simultaneously on the CEA Opteron clusters, local PC and the CRI cluster of Orsay, using one processor by job.

In order to compute MC statistical errors on $u_N(\rho)$ each total run was divided into n_B blocks and the error bar was obtained by a standard block analysis [17]. Each block involved a large number n_B^{conf} of successive MC configurations and was supposed to be

TABLE IV : $U_N(\beta)$ of the OCP as a function of β and the number of particles N . The number in bracket which corresponds to one standard deviation is the accuracy of the last digits.

| | $N = 1600$ | $N = 3200$ | $N = 6400$ | $N = 12800$ | $N = 25600$ | $N = 51200$ |
|-----|---------------|---------------|---------------|---------------|---------------|---------------|
| 0.1 | 0.20942 (7) | 0.21343 (8) | 0.21984 (8) | 0.22728 (7) | 0.23436 (7) | 0.24018 (18) |
| 0.2 | 0.32066 (7) | 0.32477 (6) | 0.32865 (4) | 0.33223 (4) | 0.33502 (4) | 0.337244 (74) |
| 0.3 | 0.385447 (36) | 0.388389 (23) | 0.391016 (23) | 0.393158 (27) | 0.394704 (25) | 0.395825 (99) |
| 0.4 | 0.430965 (23) | 0.433233 (23) | 0.435009 (19) | 0.436452 (19) | 0.437507 (18) | 0.438230 (63) |
| 0.5 | 0.465821 (16) | 0.467568 (17) | 0.468939 (17) | 0.470015 (17) | 0.470754 (15) | 0.471263 (52) |
| 0.6 | 0.493812 (13) | 0.495220 (13) | 0.496352 (16) | 0.497158 (13) | 0.497714 (13) | 0.498072 (37) |
| 0.7 | 0.517109 (13) | 0.518254 (12) | 0.519178 (12) | 0.519806 (11) | 0.520259 (13) | 0.520600 (32) |
| 0.8 | 0.536909 (8) | 0.537854 (7) | 0.538606 (9) | 0.539140 (11) | 0.539513 (11) | 0.539745 (25) |
| 0.9 | 0.554034 (10) | 0.554810 (12) | 0.555458 (8) | 0.555886 (11) | 0.556232 (10) | 0.556458 (40) |
| 1.0 | 0.569012 (15) | 0.569714 (9) | 0.570281 (8) | 0.570669 (10) | 0.570930 (9) | 0.571119 (24) |

statistically independent of the others. For each calculation we checked that the variance was independent of the size of the blocks for sufficiently large values of n_B^{conf} . Results are so stable that we shall no more discuss this point in this paper. The need of large simulations with $N = 51200$ particles appeared with the difficulty to reach the thermodynamic limit and to obtain the wanted precision for the values that we considered. But, due to huge demand in CPU time of these simulations (one month for 10000 configurations) only short chains were considered, however long enough to reach the stable plateau of the CREE and to improve the TL research (see below). Our data for $U_N(\beta)$ are reported in table IV where the number in bracket correspond to one standard deviation and represent the accuracy of the last digits and only the results for $N = 1600$ are given.

B. Connection with former simulations for $1 \leq \beta \leq 10$

Before we present our new results for $0 \leq \beta \leq 1$, we shall study the connection with the results obtained in paper I, calculated with the same MC code, but another range of values, i.e. $1 \leq \beta \leq 10$. The only difference between the two calculations, calculated in

TABLE V : Comparison with previous results of the MC energy $u_N(\beta)$ of the OCP in space S^3 in function of the number of particles N for $\beta = 5$ and $\beta = 10$. The first row, case "a", corresponds to present study and second row, case "b", to table 1 of [11]. The only difference between the two calculations is the number of configurations, typically $n_{\text{conf}} = 800 \cdot 10^6$ MC configurations after equilibration in case "a", and $n_{\text{conf}} = 5 \cdot 10^9$ in case "b". The number in bracket which corresponds to one standard deviation is the accuracy of the last digits. With two standard deviations the agreement is fulfilled.

| | N = 400 | N = 800 | N = 1600 | N = 3200 | N = 6400 | case |
|----|---------------|----------------|----------------|---------------|---------------|------|
| 5 | | :7510930 (37) | :7511501 (31) | :7512037 (35) | :7512332 (21) | a |
| 5 | :7510201 (89) | :7511042 (126) | :7511513 (135) | :7511775 (85) | | b |
| 10 | | :7998396 (26) | :7998148 (30) | :7998098 (28) | :7998043 (15) | a |
| 10 | :7998865 (53) | :7998414 (43) | :7998149 (51) | :7998131 (55) | | b |

double precision on 64 bytes work stations, is thus the maximum number of configurations, typically $n_{\text{conf}} = 800 \cdot 10^6$ MC configurations -after equilibration in previous case (case "a"), and $n_{\text{conf}} = 5 \cdot 10^9$ in this paper (case "b"). We have performed comparisons for $\beta = 1; 2; 3; 4; 5$ and $\beta = 10$. The choices retained in I were, at that time, the maximum reasonable conditions for the simulations.

Finite size effects decrease with increasing value of β . Details of CREE's for $\beta = 5$ and $\beta = 10$ are reported in Table V (N dependence of MC energy $u_N(\beta)$ in both calculations, present and I). For $\beta = 10$ the results are in good agreement. But for $\beta = 5$ slight discrepancies observed at $N = 1600$ and $N = 3200$ between the two calculations are a bit worrying. Indeed in these cases the error bars intervals do not overlap. The main reason is that, for the lowest β results of ref. I, the plateau of the CREE was in fact not reached. This feature is illustrated by figure 5 where the CREE's for $\beta = 2$ are displayed. The figure illustrates the lack of configurations in the simulations of ref. I for the CREE $U =$ versus the number of configurations, displayed for different number of particles. From top to bottom $N = 800; 1600; 3200; 6400$. The blue arrow points on the maximum number of configurations considered in I. When compared to our new calculations, clearly the Markov chain was not long enough to reach a plateau and such a drift of the CREE was probably underestimated in our previous calculations. The large variation with N of the CREE with N (solid red line)

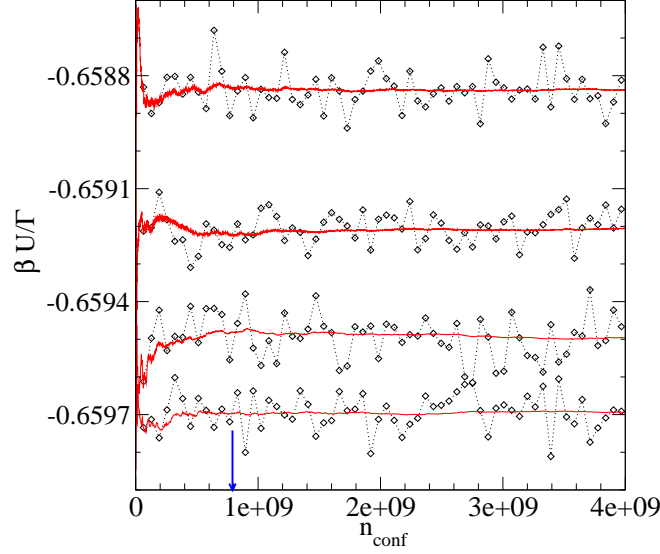


FIG. 5: Solid lines: cumulated reduced excess energy $u_N(\epsilon)$ versus the number of configurations for $\epsilon = 2$. From bottom to top $N = 800; 1600; 3200; 6400$. Symbols: block averages. The blue arrow points to the maximum number of configurations $n_{\text{conf}} = 8 \cdot 10^8$ considered in ref. I.

gives an idea of the amplitude of finite size effects. The simulation for the case $N = 6400$, not included in paper I, has been added to improve the TL extrapolation. Only the $4 \cdot 10^9$ first configurations are plotted for visibility, but clearly each CREE value reaches its equilibrium value for a fixed N value. Figure 6 illustrates how previous conclusions for the case $\epsilon = 2$ are emphasized in the case $\epsilon = 1$. It follows from the above remarks that a re-analysis of the TL of the energy of the OCP is necessary for $\epsilon = 1; 2; \dots; 10$. We recall the conclusions of I according to which the scaling law 2.4 is valid only for low ϵ and that for $\epsilon \geq 3$ the thermodynamic limit is reached more quickly with a scaling law

$$u_N(\epsilon) - u_1(\epsilon) \sim N^{-1} \text{ for } \epsilon \geq 3 \text{ and } N \gg 1 : \quad (3.2)$$

Moreover the scaling limits 2.4 and 3.2 are satisfied, depending on the value of ϵ , for very large, and sometimes prohibitive large, numbers of particles N . The ideal case would be a linear fit passing through all the points within the error bars. This situation was indeed observed by including simulations at $N = 51200$ particles and for not too low values of ϵ . In other situations we had to content ourselves with quadratic fits including the next leading order term (i.e. either $O(1/N^2)$ or $O(1/N^{4/3})$ according to the value of ϵ). In Table VI are resumed the comparisons for the TL of the energy between present and results of paper I for $\epsilon = 1; 2; 3; 4; 5; 10$. The type of the extrapolation scheme is specified in the column "fit",

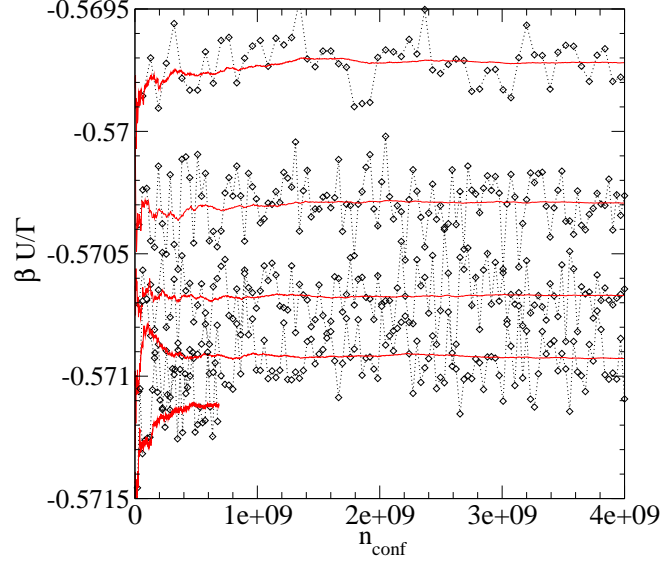


FIG. 6: Solid lines: cumulated reduced excess energy $u_N(\beta)$ versus the number of configurations for $\beta = 1$. From top to bottom $N = 3200; 6400; 12800; 25600; 51200$. Symbols: block averages.

together with the interval of N values considered for the fit. Precision are also reported. For $\beta = 5$ it is clear that results are slightly shifted between calculations. As expected for $\beta = 10$ present and previous results are similar; higher values of β should not cause any trouble.

C. Thermodynamic limit extrapolation scheme

The aim of our simulations was to compute the TL of the energy $u_{N=1}(\beta)$ with a high degree of accuracy by taking into account finite size effects which are of overwhelming importance for $\beta = 1$. The need of simulations up to $N = 51200$ and involving no less than $N = 800$, or even $N = 1600$ particles for the smallest values of β , appeared crucial to reach the scaling law 2.4. It appears that, for this range of N , MC data can be fitted with the quadratic fits

$$u_N(\beta) = u_{N=1}(\beta) + a_1 \frac{1}{N^{2=3}} + a_2 \frac{1}{N^{2=3}}^2 : \quad (3.3)$$

For most values of β it proved possible to explicitly check the asymptotic form linear in $N^{-2=3}$ (i.e. $a_2 = 0$ in equation 3.3) by keeping only the 3 largest systems, i.e. $N = 12800; 25600$ and $N = 51200$. Recall that in paper I the largest considered systems were made of $N = 3200$ particles. An exhaustive discussion follows in next section.

TABLE VI: Thermodynamic limit of the energy of the OCP versus Γ for $\beta = 1$ of, case "a", compared to previous calculations, case "b". The difference between two calculations is the maximum number of particles (no more than 3200 in case a) and the total number of configurations. The type of extrapolation scheme is specified in the column "Fit". For instance quad(3200-51200) means that a quadratic regression involving the data from $N = 3200; 6400; 12800; 51200$ has been used. The variable entering the fit is specified in the column Variable. $p \cdot 10^5$ is the precision of the fit. The number in bracket which corresponds to one standard deviation is the accuracy of the last digits.

| | $u_1 =$ | Fit | $p \cdot 10^5$ | $u_1 =$ | Fit | $p \cdot 10^5$ | Variable |
|-----|----------------|-------------------|----------------|----------------|-----------------|----------------|------------|
| | a | a | a | b | b | b | |
| 1: | 0:571387 (24) | lin (12800-51200) | 4.2 | 0:571098 (39) | cub (100-3200) | 6.9 | $N^{-2=3}$ |
| 1: | 0:571403 (22) | quad (3200-51200) | 3.8 | | | | $N^{-2=3}$ |
| 2: | 0:6598934 (68) | quad (800-6400) | 7.0 | 0:659983 (23) | quad (200-3200) | 3.5 | $N^{-2=3}$ |
| 3: | 0:7042987 (54) | quad (3200-6400) | 0.8 | 0:704348 (19) | quad (200-3200) | 2.7 | $N^{-2=3}$ |
| 4: | 0:7319760 (46) | lin (800-6400) | 0.6 | 0:731916 (12) | quad (200-3200) | 1.7 | N^{-1} |
| 5: | 0:7512608 (22) | lin (800-6400) | 0.3 | 0:7512126 (98) | quad (200-3200) | 1.3 | N^{-1} |
| 10: | 0:7997991 (16) | lin (800-6400) | 0.2 | 0:7997974 (45) | lin (400-3200) | 0.56 | N^{-1} |

D. Results for $\beta = 1$

We present and discuss in details the ten values $\Gamma = 0.1; 0.2; \dots; 1$ considered in our numerical experiments. Figures 7, 8, 9 and 10 illustrate the CREE $u_N(\Gamma)$ versus the number of configurations for several characteristic values of Γ ($\Gamma = 0.1, 0.2, 0.4$, and 0.7 respectively) typical of the different plasma regimes in the interval $(0; 1)$. Our previous comments on figures 6 and 5 (for $\Gamma = 1; 2$ respectively) are still valid in these cases. We stress once again the need of large systems together with the need of enough configurations to reach a stable plateau after thermal equilibration.

All generated configurations, $n_{\text{conf}} = 6 \cdot 10^9$, are displayed in figure 7 ($\Gamma = 0.1$) while a zoom of only the first $2 \cdot 10^9$ configurations is displayed in figure 8 ($\Gamma = 0.2$), which exemplifies the plateau reached by the CREE for $N = 51200$. On the last two figures 9 and 10, respectively for $\Gamma = 0.4$ and $\Gamma = 0.7$ and $n_{\text{conf}} = 4 \cdot 10^9$, we see the good convergence with

TABLE V II: Thermodynamic limit of the energy of the OCP versus Γ . The number in bracket which corresponds to one standard deviation is the accuracy of the last digits. The type of extrapolation scheme is specified in the column "fit". The variable entering the fit is $N^{-2/3}$.

| | $u_1 =$ | Fit |
|-----|---------------|-------------------|
| 0:1 | 0.25117 (34) | quad (6400-51200) |
| 0:2 | 0.34111 (17) | quad (6400-51200) |
| 0:3 | 0.397693 (64) | quad (3200-51200) |
| 0:4 | 0.439323 (53) | lin (12800-51200) |
| 0:4 | 0.439528 (50) | quad (3200-51200) |
| 0:5 | 0.472028 (45) | lin (12800-51200) |
| 0:5 | 0.472172 (42) | quad (3200-51200) |
| 0:6 | 0.498663 (38) | lin (12800-51200) |
| 0:6 | 0.498715 (21) | quad (1600-51200) |
| 0:7 | 0.521063 (32) | lin (12800-51200) |
| 0:7 | 0.521064 (20) | quad (1600-51200) |
| 0:8 | 0.540146 (28) | lin (12800-51200) |
| 0:8 | 0.540173 (15) | quad (1600-51200) |
| 0:9 | 0.556823 (30) | lin (12800-51200) |
| 0:9 | 0.556801 (25) | quad (3200-51200) |
| 1:0 | 0.571387 (24) | lin (12800-51200) |
| 1:0 | 0.571403 (22) | quad (3200-51200) |

N as the interval width between CREE values decreases from top to bottom. By contrast the low Γ runs do not exhibit this regular decrease. Of course beyond visual impressions only the possibility and precision of the fitting process of the MC CREE results will give a firm answer on the quality of the TL calculation for each Γ value.

Table IV resumes present work MC calculations of the MC energy $u_N(\Gamma) =$ of the OCP as a function of Γ for $N = 1600$ to $N = 51200$. The number in bracket which corresponds to one standard deviation is the accuracy of the last digits. Results corresponding to $N = 1600$, not included in the fits, are not reported. The thermodynamic limit values of the energy versus Γ are reported in Table V II. The type of extrapolation schemes retained

in the fits, i.e. linear or quadratic (cf equation 3.3), are specified. In figures 11, 12, 13 and 14 we display the quadratic fit of $u_N(\rho)$ (solid black line) and the linear fits for the 3 largest numbers of particles considered, when available (red dashed line) for $\rho = 1, 0.7, 0.4$, and $\rho = 0.1$ respectively. The error bars on the value of the TL of the energy $u_1(\rho)$ reported in table V II are the error bars of the linear (or quadratic) regression.

We discuss now the results from high to low ρ 's. Figure 11 illustrates the high quality of the fits obtained in the case $\rho = 1.0$. Indeed the extrapolated TL of $u_N(\rho)$ coincide for both the linear and the quadratic fits (the latter involving more states with low number of particles and the former only the 3 largest systems) with a nice overlap of the error bars. Results are similar down to $\rho = 0.7$, as illustrated in Figure 12 for $\rho = 0.7$.

In the range $0.5 \leq \rho \leq 0.7$ the precision of the fits is good but the linear and the quadratic fit extrapolations do not give exactly the same TL values, however the error bars do overlap. Figure 13, corresponding to the case $\rho = 0.4$, illustrates the smallest ρ at which a linear fit is possible with the 3 higher values of N . The linear and the quadratic fit extrapolations giving the TL values would coincide within the error bars if the latter were defined to be two standard deviations rather than only one according to our choice.

For smaller or equal to 0.3 it was impossible to reach an asymptotic form of $u_N(\rho)$, linear in the variable $N^{-2/3}$, and only a quadratic polynomial fit was possible (cf table V II). For that reason it is legitimate to consider the error bars on the extrapolated value $u_1(\rho)$ as overoptimistic in this range of ρ , see figure 14 for an illustration in the case $\rho = 0.1$. Simulations involving larger numbers of particles would be necessary but are out of our reach.

For all the states with a $\rho \geq 0.4$ the TL limit $u_1(\rho)$ can thus be obtained with a high precision $\pm 10^{-5}$, after a careful study of finite size effects on the MC energies $u_N(\rho)$. For smaller values of ρ , for instance $\rho = 0.1$, samples of more than $N \sim 200000$ particles should be used to reach the leading order of the asymptotic regime 2.4. However such an effort would be useless since HNC and Cohen approximations are then "exact" within the wanted precision on u . The $u_1(\rho)$ are perfectly well fitted in the range $0.4 \leq \rho \leq 1$ by the Cohen's functional form, given by equation 2.1a, involving the five parameters p_i ($i = 0, \dots, 4$) given in table I.

IV . C O N C L U S I O N

In this conclusion we compare at first the Cohen-O rtner low expansions, HNC and MC data. Figure 3 shows without ambiguity the good agreement between HNC and MC results in the range $0 \leq \beta u_N \leq 1$ and the large departure of both results with analytical expansion ones, DH (for $\beta u_N \leq 0.05$), Th1 (for $\beta u_N \leq 0.3$) and Th2 (for $\beta u_N \leq 0.2$). Note however that the scale of the figure is not large enough to discriminate between HNC and MC results, notably because the errors bars on MC results are smaller than the size of the symbols. A more enlightening illustration is that of figure 2 which gives the ratio of the MC and HNC energies. The disagreement for $\beta u_N \leq 0.3$ results from a bad evaluation of the TL of u_N due to huge finite size effects spoiling the MC data, while the disagreement for $\beta u_N \leq 0.6$ simply reflects the failure of the HNC approximation at high βu_N . A nearly perfect agreement between MC and HNC results, compatible with one standard deviation is observed only at $\beta u_N = 0.5$; with two standard deviations the HNC results are within the error bars of the MC data in the interval $0.4 \leq \beta u_N \leq 0.6$. By passing our new HNC calculations for some values of βu_N in the range $(1;10)$ are plotted in figure 4 where MC data were also included for comparison.

It is the place to resume our analysis. We found that, for a wanted precision of $p = 10^{-5}$ on the energy :

$0 \leq \beta u_N \leq 0.05$ is the range of validity of Debye-H uckel theory.

$0 \leq \beta u_N \leq 0.3$ is the range of validity of Cohen low expansion 2.1.

O rtner's additional terms do not improve the results.

$0 \leq \beta u_N \leq 0.5$ is the range of validity of HNC . The data are perfectly represented by the eight parameters βu_N of tables I and II.

We were able to extract the thermodynamic limit of the OCP energy from our MC simulations with a precision not smaller than $p = 10^{-5}$ in the range $0.4 \leq \beta u_N \leq 1$. Our data are well fitted by the five parameters βu_N of table I.

-
- [1] M .Baus and J.P .Hansen, Phys.Rep. 59, 1 (1980).
- [2] P.E .Debye, E .Huckel Physikalische 24, 185 (1923).
- [3] E.G .D .Cohen and T .J.M urphy, The Phys.of Fluids 12, 1404 (1969).
- [4] J.O rtner, Phys.Rev.E 59, 6312 (1999).
- [5] K .C .Ng, J.Chem .Phys. 61, 2680 (1974).
- [6] S.G .Brush, H.L.Sahlin, and E .Teller, J.Chem .Phys. 45, 2102 (1966).
- [7] E.L.Pollock and J.P .Hansen, Phys.Rev.A 8, 3110 (1973).
- [8] W .L.Slattery, G .D .Doolen, and H.E .DeW itt, Phys.Rev.A 26, 2255 (1982).
- [9] H.E .DeW itt, Proceedings of the International conference on Strongly Coupled Coulomb Systems (Boston, 1997).
- [10] J.M .Caillol, J.Chem .Phys. 111, 6528 (1999).
- [11] J.M .Caillol, J.Chem .Phys. 111, 6538 (1999).
- [12] J.M .Caillol and D .G illes, J.Stat.Phys. 100, 933 (2000).
- [13] Stratonovich R L, Sov.Phys.Solid State 2, 1824 (1958).
- [14] Hubbard, J 1954 Phys.Rev.Lett. 3, 77 (1954); Hubbard J and Shoenfeld P 1972 Phys.Lett. A 40, 245 (1972).
- [15] J.M .Caillol and J.L.Rambault, J.Stat.Phys. 103, 753 (2001).
- [16] F.H .Stillinger and R .Lovett, J.Chem .Phys. 49, 1991 (1968).
- [17] D .Frenkel and B .Sm it, Understanding Molecular Simulation (Academic, New York, 1996).

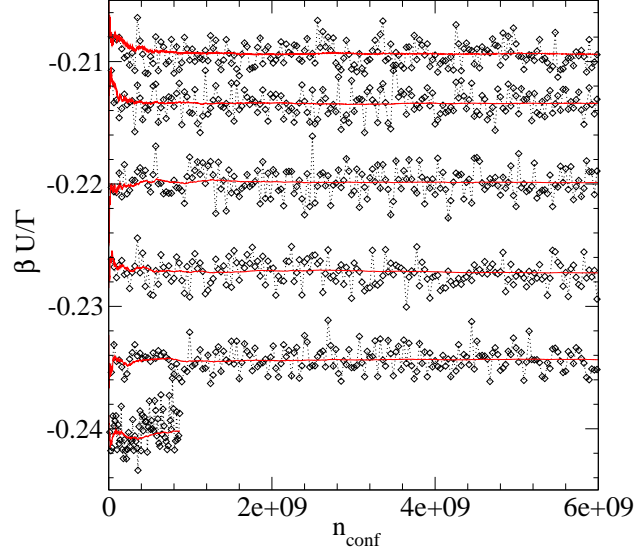


FIG .7: Solid lines: cum ulated reduced excess energy $u_N(\beta) =$ versus the num ber of con gurations for $\beta = 0.1$. From top to bottom $N = 1600; 3200; 6400; 12800; 25600; 51200$. Symbols: block averages.

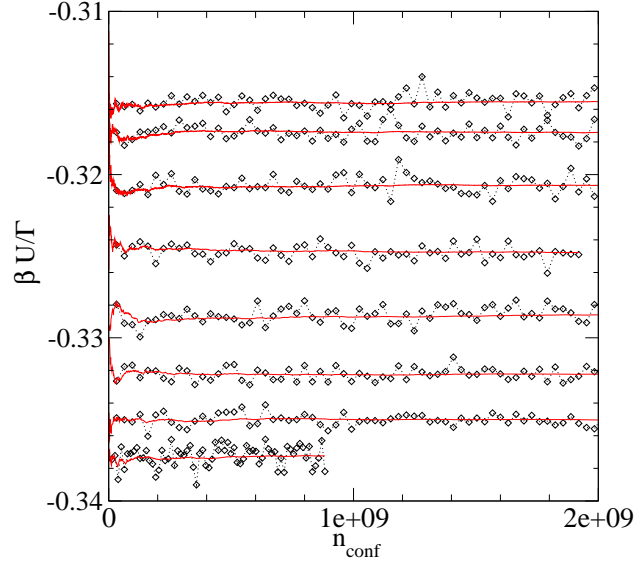


FIG .8: Solid lines: cum ulated reduced excess energy $u_N(\beta) =$ versus the num ber of con gurations for $\beta = 0.2$. From top to bottom $N = 400; 800; 1600; 3200; 6400; 12800; 25600; 51200$. Symbols: block averages.

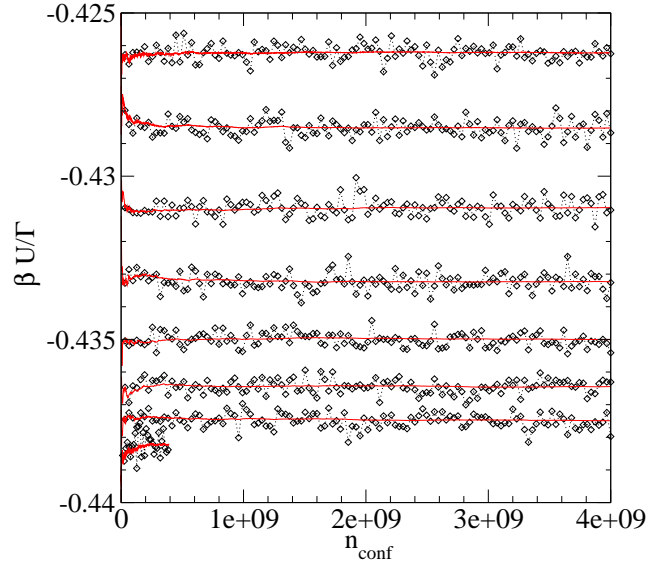


FIG .9: Solid lines: cumulated reduced excess energy $u_N(\eta)$ versus the number of configurations for $\eta = 0.4$. From top to bottom $N = 400; 800; 1600; 3200; 6400; 12800; 25600; 51200$. Symbols: block averages.

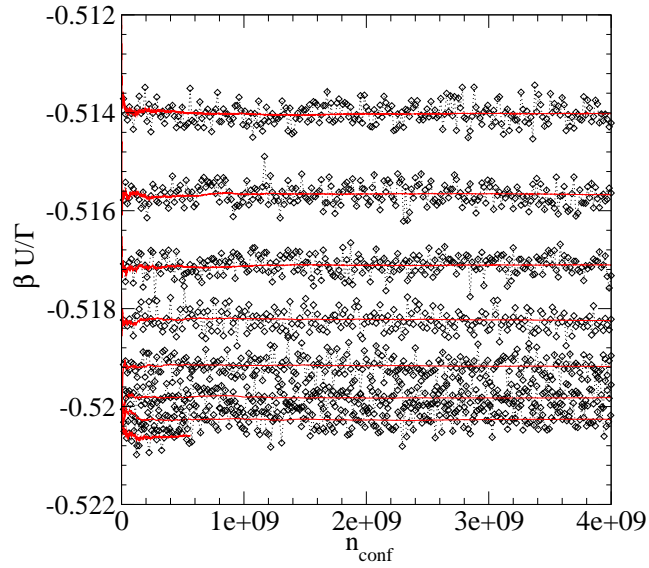


FIG .10: Solid lines: cumulated reduced excess energy $u_N(\eta)$ versus the number of configurations for $\eta = 0.7$. From top to bottom $N = 400; 800; 1600; 3200; 6400; 12800; 25600; 51200$. Symbols: block averages.

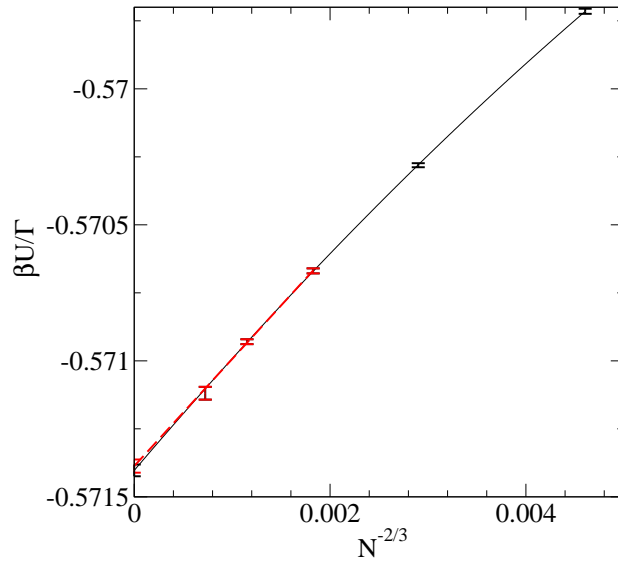


FIG. 11: Solid lines: cumulated reduced excess energy $u_N(\beta) = \beta U/\Gamma$ versus $N^{-2/3}$ for $\beta = 1$. From left to right $N = 1; 51200; 25600; 12800; 6400; 3200$. The error bars correspond to one standard deviation. Solid black line: quadratic polynomial regression of MC data. Dashed red line: linear regression of the 3 larger systems MC data.

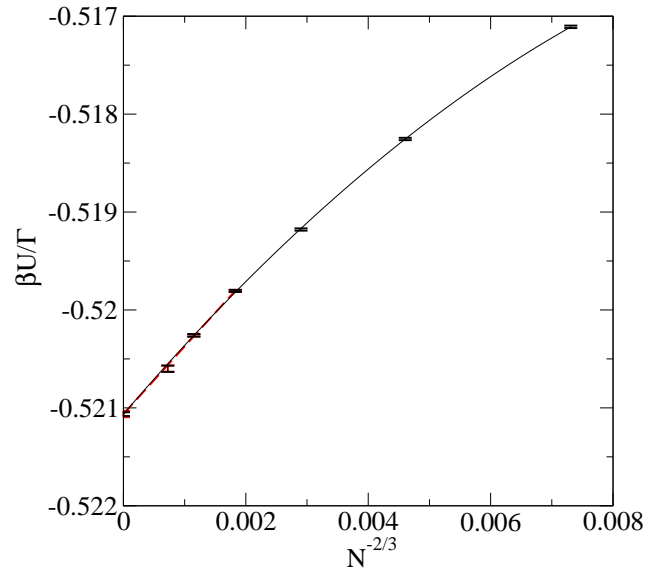


FIG. 12: Same legend than figure 11 but for $\beta = 0.7$. From left to right $N = 1; 51200; 25600; 12800; 6400; 3200; 1600$.

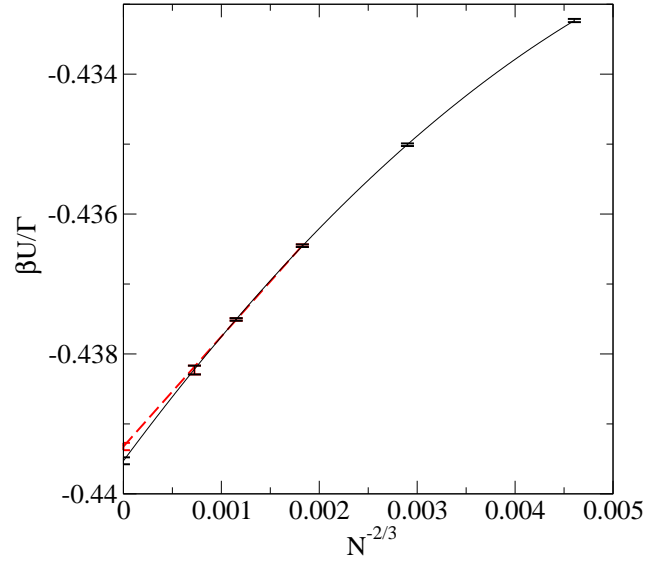


FIG. 13: Same legend than figure 11 but for $\beta = 0.4$. From left to right $N = 1 ; 51200; 25600; 12800; 6400; 3200$.

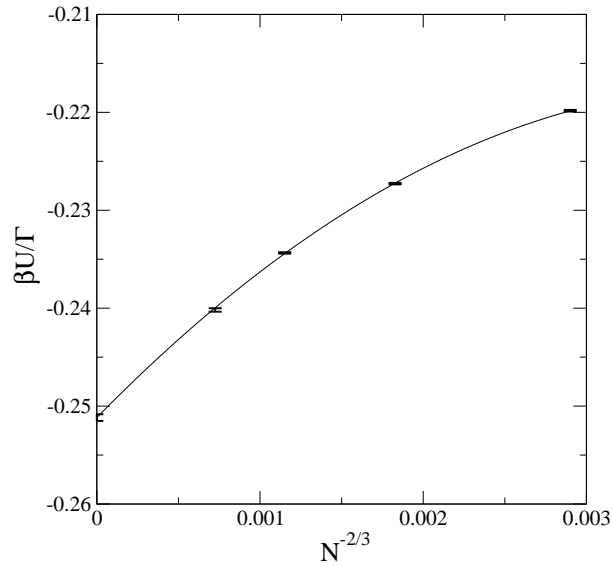


FIG. 14: Solid lines: cumulated reduced excess energy $u_N(\beta) = \beta U/T$ versus $1/N^{2/3}$ for $\beta = 0.1$. From left to right $N = 1 ; 51200; 25600; 12800; 6400; 3200$. The error bars correspond to one standard deviation. Solid black line : quadratic polynomial regression of MC data.